Measurement report: Six-year DOAS observations reveal post-2020 rebound of ship SO₂ emissions in a Shanghai port despite low-sulfur fuel policies

Jiaqi Liu¹, Shanshan Wang^{1,2}, Yan Zhang^{1,2,4,5}, Sanbao Zhang¹, Yuhao Yan¹, Zimin Han¹, Bin Zhou^{1,2,3}

Shanghai Key Laboratory of Atmospheric Particle Pollution and Prevention (LAP3), Department of Environmental Science and Engineering, Fudan University, Shanghai, 200438, China

Abstract. The expansion of maritime trade has made ship emissions a significant target for SO₂ reduction policies. However, there is still a lack of observational data to reflect the long-term changes in SO₂ emission from ships. This study conducted continuous observational experiments using Differential Optical Absorption Spectroscopy (DOAS) from 2018 to 2023 in a shipping channel in Shanghai, China. By employing machine learning and background subtraction, the trends of ambient SO₂ related to ship emissions (Ship_related_SO₂) over the six-year period were revealed. Furthermore, whether ships in the channel were using low-sulfur fuels was determined by a decomposition of SO₂-rich plumes signals (which reflect high-emission ships) and baseline variations. The findings indicate that ship activities increased ambient SO₂ concentrations in the channel by 0.48 ± 0.25 ppbv (43.24% of urban background levels). During the policy adjustment phase (2018 to 2020), Ship_related_SO₂ levels declined steadily due to low-sulfur fuel regulations. While from 2021 to 2023 (the policy stabilization phase), increased ship activity became the dominant driver of rising Ship_related_SO₂ levels. Despite policy effectiveness, excessive emissions from cargo ships persisted throughout the study period. This study quantified the contribution of ship emissions to ambient SO₂ during 2018–2023 based on observations, evaluating the effectiveness of low-sulfur policies and supporting ongoing efforts to mitigate SO₂ pollution from maritime activities. The methodology developed here can be adapted to other global shipping channels, providing a framework for monitoring and regulating ship emissions worldwide.

1 Introduction

Sulfur dioxide (SO₂), classified as an airborne carcinogen (Von Nieding, 1978; Ghanbari Ghozikali et al., 2016), contributes to urban haze, increases environmental health risks, and facilitates the formation of sulfate aerosols through heterogeneous

²Institute of Eco-Chongming (IEC), Shanghai, 202162, China

³Institute of Atmospheric Sciences, Fudan University, Shanghai, 200438, China

⁴National Observations and Research Station for Wetland Ecosystems of the Yangtze Estuary, Fudan University, Shanghai 200438, China

⁵Institute of Digitalized Sustainable Transformation, Big Data Institute, Fudan University, Shanghai 200433, China *Correspondence to*: Bin Zhou (binzhou@fudan.edu.cn) and Shanshan Wang (shanshanwang@fudan.edu.cn)

reactions (Squizzato et al., 2018). Although volcanic eruptions are a major natural source of SO₂ (Carn et al., 2016), the widespread use of sulfur-containing fuels, such as coal and oil, in human activities remains the dominant anthropogenic source globally (Zhong et al., 2019; Van Aardenne et al., 2001). In response to the global challenge of rising energy demand and continued SO₂ emissions, the United States (Miller, 2011), the European Union (Meyer and Pac, 2017), and several other countries (Moran, 2007; Lou et al., 2021; Kuttippurath, 2022) have introduced a series of policies that have effectively reduced land-based SO₂ emissions. However, with the rapid expansion of maritime trade, SO₂ emissions from shipping are projected to keep increasing (Zhao et al., 2020), posing growing threats to coastal atmospheric environments (Zhang et al., 2017; Wang et al., 2019), and becoming a major focus of global research and policy initiatives.

To curb SO₂ emissions from maritime shipping, the International Maritime Organization (IMO) implemented a global regulation in 2020 that reduced the allowable sulfur content from 3.5% to 0.5% (Zhao et al., 2020; Fossum et al., 2024), aiming to reduce the shipping industry's impact on atmospheric environments. In addition, six Emission Control Areas (ECAs) have been established worldwide. Among them, the Baltic Sea, North Sea, North American, and U.S. Caribbean ECAs receiving IMO approval, while the European and California coastal ECAs were independently designated by their respective authorities (Fossum et al., 2024; Mohiuddin et al., 2024). As the world's most active maritime trading nation (Ducruet and Wang, 2018), China's port activities exert a particularly strong influence on coastal air quality. In 2015, China launched its Domestic Emission Control Area (DECA 1.0) policy, requiring ships with compatible facilities in the Pearl River Delta, Yangtze River Delta, and Bohai Rim (Beijing-Tianjin-Hebei) regions to use fuel with ≤0.5% sulfur content during berthing periods from January 2016 (Zou et al., 2020; Zhang et al., 2019; Wang et al., 2021). By late 2018, China 50 upgraded the policy to DECA 2.0, mandating that all ships operating within China's territorial sea (12-nautical-mile zone) must use fuel with \le 0.5\% sulfur content while sailing from January 2019 onward, and <0.1\% sulfur content while at berth. or adopt equivalent emission control measures. For example, installing exhaust gas cleaning systems (scrubbers) (Lunde Hermansson et al., 2024; Andreasen and Mayer, 2007), adopting alternative fuels like LNG(Paylenko et al., 2020; Attah and Bucknall, 2015), methanol(Svanberg et al., 2018; Shi et al., 2023) and biofuels(Cesilla De Souza and Eugênio Abel Seabra, 2024; Ahmed et al., 2025), and applying operational strategies such as slow steaming and shore power use(Zis et al., 2015; 55 Zis et al., 2014). Despite the effectiveness of these policy measures in controlling SO₂ emissions from shipping, previous studies have shown that the impact of ship emissions on air quality in coastal areas is still significant (Viana et al., 2014; Xiao et al., 2022; Xiao et al., 2023), which provides an important basis for further research on reduction of ship SO₂ emissions.

Previous research has extensively utilized high spatiotemporal resolution AIS (Automatic Identification System) ship activity data and air quality models to quantify the environmental impact of ship emissions (Zhao et al., 2020; Liu et al., 2017; Feng et al., 2019a; Li et al., 2020; Fan et al., 2016; Zhang et al., 2023; Feng et al., 2023). Simulation results from 2016 to 2020 show that the control of SO₂ emissions from ships was particularly effective in 2020 due to the influence of low-sulfur policies (Luo et al., 2024). Compared to simulations, observational data can more accurately capture real-world

changes in pollution from ships and ports (Eger et al., 2023), while also serving as a critical tool for refining emission inventories, improving atmospheric models, and identifying excessive emission ships (Cheng et al., 2019; Liu et al., 2024; Krause et al., 2021; Kattner et al., 2015). In light of the low-sulfur policies, critical questions remain: Has the low-sulfur policy effectively regulated ship SO₂ emissions? Can the low levels of SO₂ observed in 2020 be sustained amidst anticipated long-term growth in maritime activity? Addressing these questions requires continued observational research.

This study aims to address these gaps by presenting long-term observational data from the Shanghai shipping channel, one of the busiest maritime routes in the world. By integrating Differential Optical Absorption Spectroscopy (DOAS) measurements with machine learning, we propose a novel approach to quantifying ship emissions and evaluating policy effectiveness, with implications for other coastal regions facing similar challenges. Specifically, this study pursues three key objectives: (1) to quantify the contribution of ship emissions to ambient SO₂ levels in the Shanghai shipping channel over a six-year period (2018–2023), (2) to evaluate the effectiveness of low-sulfur policies in reducing ship-related SO₂ emissions, and (3) to identify potential gaps in current emission inventories and regulatory frameworks.

2 Data and methods

2.1 DOAS set up and spectra retrieval

Experiments measuring SO₂ were conducted using two active DOAS systems from 2018 to 2023 at Wusong wharf (WSW, 31.37 N,121.51 E) and the Jiangwan Campus of Fudan University (FDU, 31.34 N, 121.51 E). The WSW site is located downstream the confluence of the Huangpu River and the Yangtze River, where over a thousand vessels pass daily, including cargo ships, passenger ships, fishing boats, oil tanker and other ships in various operating conditions. Shipping activities are the primary source of ambient pollution at this site. Fig. S1, S2 and Text S1 give an overview of ship activity in the WSW Channel. The FDU site, situated 4 km southwest of WSW, characterized as a typical urban location with no significant local pollution sources, as noted in previous study (Liu et al., 2024; Guo et al., 2020).

Each active DOAS system was equipped with a light source (150 W xenon lamp), a reflecting/receiving telescope, an array of retroreflectors, a spectrometer, and a computer. In WSW, the light was emitted from a laboratory on the third floor (approximately 10 meters above ground level) of the Wusong Maritime Safety Administration building (ground elevation ~6 m above sea level) and reflected across the channel by an array of retroreflectors located on the opposite bank (which is also about 10 meters above ground level), forming a light path of 1,540 m. Given the local tidal range of approximately 1-4 meters, the vertical height of the light path above the water surface varied between roughly 12 and 15 meters. Due to the optical path crossing the airspace above the shipping channel, emission signals from vessels below can be easily captured by active DOAS. At FDU, the transmitting terminal of active DOAS was located in a laboratory on the 7th floor of the Environmental Science Building, with the retroreflectors array placed to the southwest, forming a light path of 2,689 m. In previous studies, this site effectively represents Shanghai's urban areas with relatively clean atmospheric conditions (Liu et

al., 2024; Zhu et al., 2020; Gu et al., 2022). Spectral signals retrieval and time-series pollutant concentrations calculations were performed using the DOASIS software developed by the Institute of Environmental Physics at Heidelberg University, with SO₂ retrieved in the 299~308 nm wavelength range. Additional technical details on the DOAS instrument, spectral data processing, and detection limits are available provided in Text S2 and Table S1 of the Supporting Information.

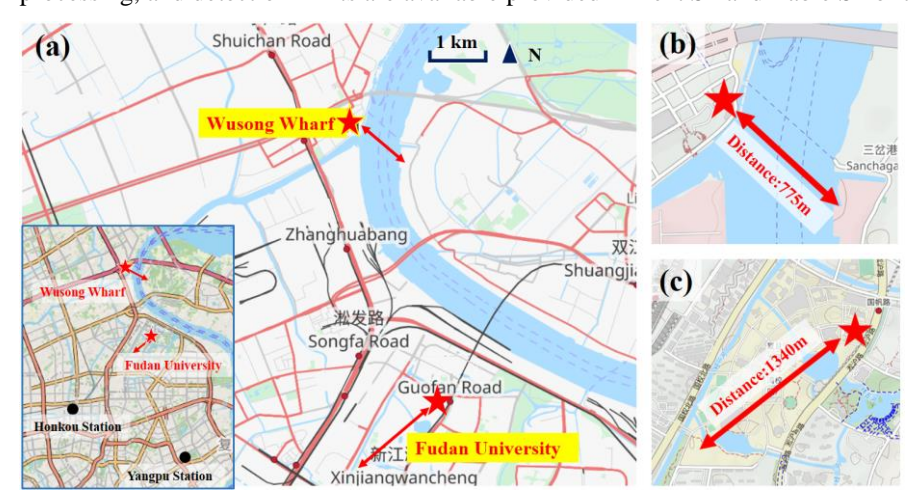


Figure 1: Location of the relevant site in this campaign. (a) The red pentagon represents the location of DOAS in Wusong Wharf (WSW) and Fudan University (FDU), respectively; the bidirectional arrows indicate the light path of DOAS. The black circles represent the two environmental monitor stations around FDU station. (b) DOAS light path setting in WSW, and (c) in FDU. Base map: © OpenStreetMap contributors, licensed under ODbL.

2.2 Machine learning and Ship related SO₂ obtained

100

105

110

115

The SO₂ in the atmosphere associated with ship activity in the channel (Ship_related_SO₂) was obtained by removing both meteorological effects and land-based emissions from the completed WSW observations, as shown in Fig. 2. Therefore, this study developed two data-processing models using extremeGradientBoostingRegressor (XGB) and ExtraTreesRegressor (ETR). The first model was used to impute missing SO₂ concentration data (Fig. 2a), while the second model was designed to eliminate meteorological influences (Fig. 2b). Both models used machine learning techniques to capture complex relationships among multiple variables and improve data accuracy.

XGB was selected to address data gaps from 2018 to 2023 caused by weather conditions and equipment maintenance at both two sites, XGB is an optimized distributed gradient enhancement library designed for efficiency, flexibility, and portability. It implements machine learning algorithms in the Gradient Boosting framework (Pan, 2018; Friedman, 2002). These models identify patterns between feature and target vectors in large datasets to make predictions or decisions, and they have been maturely applied to environmental research (Li et al., 2024; Zhu et al., 2022; Zhang et al., 2022).

As illustrated in Fig. 2a, the gap-filling model for WSW SO₂ incorporates several predictive features representing three major types of environmental influences: including meteorological conditions, ship emissions, and urban land-based emissions. Specifically, co-measured pollutants at WSW (NO₂, HCHO, HONO, O₃) help represent shipping-related

emissions through cross-species learning, while SO₂ measured at FDU—after meteorological normalization (Deweathered_FDU)—accounts for urban land-based emission influences. When filling gaps in the FDU SO₂, NO₂ concentration from active DOAS in FDU, and SO₂ from two surrounding environmental monitoring stations, are used to represent environment characteristics of land emissions in Shanghai. Besides, seven meteorological factors, including temperature (TEMP), relative humidity (RH), wind speed (WS), wind direction (WD), solar radiation (SSRD), boundary layer height (BLH), and surface pressure (P) from the European Center for Medium-Range Weather Forecasts (ECMWF) atmospheric reanalysis product ERA5, were used as meteorological impacts for both models. Observed_WSW and Observed_FDU represent the completed SO₂ sequence after XGB filling. All input data were hourly averages. Models were trained with 5-fold cross-validation and evaluated through independent validation test. The details about Machine learning data input, model tuning, and performance evaluation can be seen in Text S3.

130 The Deweathered model is used to eliminate the influence of meteorological factors on air pollution. This method simulates and offsets the impacts of various meteorological conditions, thereby estimating pollutant concentrations independent of weather variability (Vu et al., 2019; Grange et al., 2018). Among the commonly used methods, tree-based ensemble learning models, such as Random Forest and its variants, have been widely applied and proven effective in deweathering air quality data (Grange and Carslaw, 2019; Grange et al., 2018; Ceballos-Santos et al., 2021). To the best of our knowledge, this study is the first to apply the ETR specifically for deweathering Ship_related_SO₂ data. In this study, the ETR model was selected as the core algorithm. ETR is a variant of the Random Forest model, sharing nearly identical ensemble learning principles but introducing greater randomness during node splitting. This added randomness helps further reduce model variance and overfitting risk compared to standard RF, while maintaining comparable interpretability and robustness (Gall et al., 2011). For both sites, a large amount of historical meteorological data from ERA5 reanalysis dataset and time-related variables (Unix time, Julian day, and day of the week) were put into Deweathered model training. The training process and parameter description of the model are provided in Fig. S7 and Text S3 of the Supporting Information.

By applying Deweathered model to the observed SO₂ at WSW and FDU in Fig. 2b, c, the study isolated the ambient SO₂ contribution directly attributable to ship emissions (Ship_related_SO₂). This is because after accounting for meteorological effects, the SO₂ concentrations recorded at WSW reflect the combined influence of the urban land-based emissions and ships emissions. For the FDU site, however, the Deweathered model effectively removes the influence of transported pollution under different wind directions (Fig. S8)—for example, ship-related SO₂ transported from the northeast channel—so that the residual values can represent the locally generated SO₂ level. Given that both FDU and WSW are located in similar environments, primarily surrounded by residential areas and typical urban roads, the Deweathered_SO₂ concentrations at FDU are therefore taken as the background level for Shanghai's urban region. Thus, by subtracting the background (Deweathered_FDU) from the Deweathered_WSW, the contribution of Ship_related_SO₂ can be effectively determined.

145

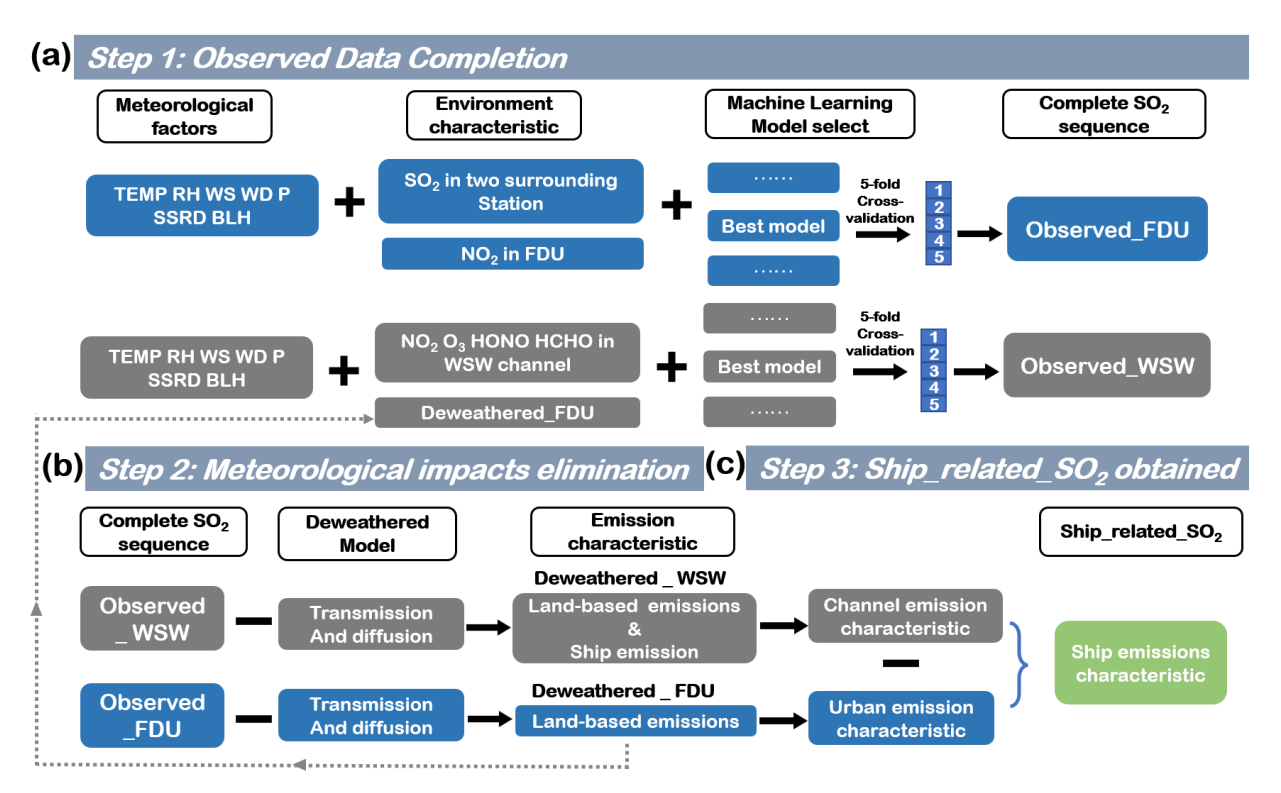


Figure 2: Schematics of Ship_related_SO₂ obtained based on DOAS observation, machine learning and meteorological impacts elimination (a) To complete the observation sequence, several models were trained and the most effective XGB model was selected, using 5-fold cross-validation. For the training of FDU, the feature parameters were selected from the continuous observation data of two automatic monitoring stations near FDU and seven meteorological data. The training of WSW used the SO₂ observation data of FDU, other pollution data observed in the channel and seven meteorological data. (b) Eliminate meteorological influences on Observed_WSW and Observed_FDU to highlight local emission impacts. (c) Subtracting the emission characteristics of FDU and WSW to obtain Ship_related_SO₂.

2.3 Auxiliary data

155

This study utilized AIS-based ship trajectory data to identify suspicious high-emission ships. AIS data provide detailed real-time information on ship locations, speeds, routes, and types, having been widely used in the study of ship emissions and related environmental impacts (Yang et al., 2019; Tu et al., 2018). The automatic monitoring stations for ambient air quality, Yangpu Station and Hongkou Station, provided hourly SO₂ concentration time series data from 2018 to 2023, which were used as input variables for imputing missing values in Observed_SO₂. All meteorological data used in this study were obtained from the fifth-generation European Centre for Medium-Range Weather Forecasts (ECMWF) atmospheric reanalysis, known as ERA5, which provides hourly around-the-clock meteorological factors from surface up to 0.01 hpa with the spatial resolution of 0.25 °× 0.25 (Marshall, 2000; Hersbach et al., 2020).

3 Results and Discussion

180

185

3.1 Long-Term Characteristics of SO₂

Figure 3 illustrates the monthly variations in SO₂ concentrations at the FDU background site and the WSW shipping channel site from 2018 to 2023, both before and after Deweathered. At the FDU site (Fig. 3a, b), the observed SO₂ concentrations display significant variability and weak inter-annual correlation, indicative of the influence of meteorological factors. After Deweathered, the SO₂ levels demonstrate a highly consistent trend over the six years, with minimal inter-annual differences. This reflects the stable nature of land-based emissions and highlights the effectiveness of the Deweathered process in isolating anthropogenic emission signals from meteorological noise. In contrast, at the WSW site (Fig. 3c, d), the Deweathered model also reduces variability and enhances the stability of the annual trends compared to the observed data. However, noticeable differences remain between years, likely due to the irregular and dynamic nature of shipping activities.

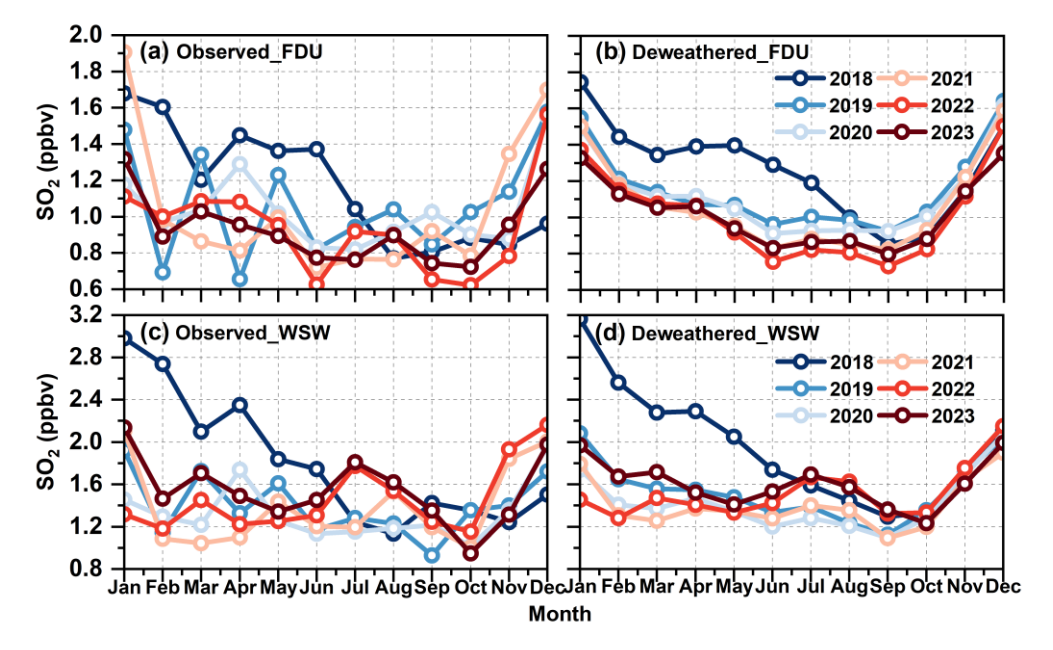


Figure 3: Monthly SO₂ concentrations at the FDU background site and WSW shipping channel site from 2018 to 2023. (a) observed and (b) meteorological impacts eliminated (deweathered) SO₂ concentrations at the FDU site, respectively. (c) and (d): the corresponding data for the WSW site.

Figure 4 shows the observed monthly average SO_2 concentrations at WSW and FDU from 2018 to 2023, as well as the results after removing meteorological influences. Table 1 presents their annual changes. Figure S9 displays their annual changes by a column chart. Influenced by the activities of ships using sulphur-containing fuels in the channel, the observed SO_2 in WSW (Observed_WSW) was notably higher than the observed SO_2 in FDU (Observed_FDU), with mean values of 1.49 ± 1.25 ppbv and 1.03 ± 0.88 ppbv, respectively. Owing to China's relentless efforts to improve air quality and reduce the use of sulphur-containing fuels, including initiatives such as the Air Pollution Prevention and Control Action Plan (2013–2017) and the Three-Year Action Plan to Fight Air Pollution (2018–2021) (Yue et al., 2020; Cai et al., 2017; Feng et al.,

2019b), the Observed FDU have decreased to relatively low levels and have shown a continuous decline over the past six years, with a 19.0% (0.22 ppby) reduction from 2018 to 2023. Conversely, the Observed WSW showed an annual trend of first decreasing by 26.11% from 2018 to 2020, reaching their lowest point in 2020, followed by a gradual increase of 16.5% from 2020 to 2023. This trend before 2020 is consistent with previous studies (Luo et al., 2024). Both locations exhibit a pattern of slightly higher SO₂ concentrations in winter and lower concentrations in summer, with fluctuations occurring midyear. Emissions and meteorological conditions are the two primary factors influencing atmospheric pollutant levels (Zhao et al., 2020). Changes in SO₂ emissions serve as the primary driving force. According to the Multi-resolution Emission Inventory for China (MEIC), residential and transportation sources of SO₂ emissions in Shanghai are significantly higher in winter than in other seasons (Fig. S10), likely contributing to the elevated winter values. The transport and dispersion of SO₂ from other sources under specific wind directions, such as emissions from power generation activities located far from the WSW and FDU sites, may account for the mid-year fluctuations in SO₂ concentrations. We trained 50 ETR models on bootstrap samples of the training data for each site and computed the permutation importance (with 95% confidence intervals) for each predictor variable. The result shows that "wind direction" became the most important variable for explaining SO₂ variability at both sites (Fig. S11), which aligns with the findings of Grange and Carslaw (2019) at the port city of Dover in England. The higher degree of fluctuation at WSW compared to FDU can be attributed to the more irregular ship emissions at WSW. Fig. S12 shows the overall increasing trend in the number of ships from 2018 to 2023, with irregular fluctuations within each year. In addition, a ship emission inventory based on AIS data was constructed, which further supports the interpretation of the variability observed at WSW (Text S5). Furthermore, the cold and dry winter monsoon reduces the rates of SO₂ oxidation and wet deposition, resulting in a longer lifetime of SO₂ molecules and thus easier accumulation. In contrast, during the summer, increased chemical reactivity and more effective wet removal processes lead to lower SO₂ concentrations.

190

195

200

205

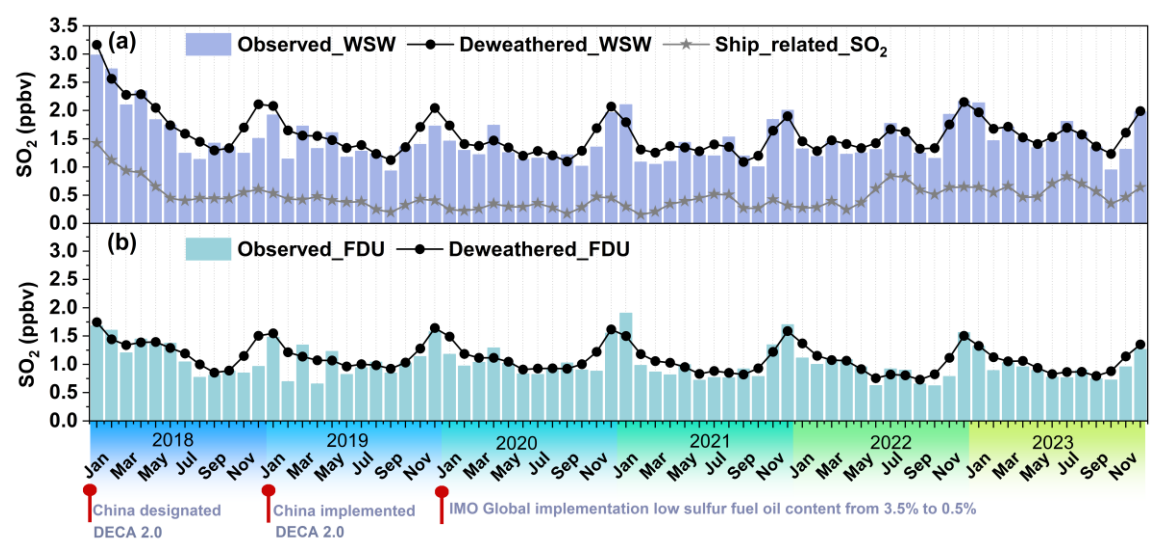


Figure 4: Monthly Observed_SO₂ concentrations based on DOAS and Deweathered_SO₂ after weather normalization in WSW and FDU, and Ship_related_SO₂ contributions during 2018-2023. (a) The light purple bars represent the monthly average Observed_SO₂ concentration at WSW; The solid black circles represent the deweathered SO₂ concentration at WSW after removing meteorological influences. The gray star symbols indicate the monthly average contribution of Ship_related_SO₂. (b) The light blue bars represent the monthly average observed SO₂ concentration at FDU; The solid black circles represent the Deweathered_SO₂ concentration at FDU removing meteorological influences.

Table 1: The annual concentration of Observed_WSW, Deweathered_WSW, Observed_FDU, Deweathered_FDU and Ship_related_SO₂ from 2018 to 2023.

SO ₂ (ppbv)	2018	2019	2020	2021	2022	2023
Observed_WSW	1.80 ± 1.75	1.40 ± 1.23	1.33 ± 1.03	1.40 ± 1.29	1.46 ± 1.04	1.55 ± 0.96
Deweathered_WSW	1.96 ± 0.56	1.54 ± 0.32	1.43 ± 0.29	1.41 ± 0.26	1.52 ± 0.27	1.60 ± 0.25
Observed_FDU	1.16 ± 1.04	1.07 ± 0.84	1.04 ± 0.82	1.04 ± 0.99	0.94 ± 0.81	0.94 ± 0.74
Deweathered_FDU	1.27 ± 0.29	1.16 ± 0.26	1.12 ± 0.25	1.07 ± 0.28	1.01 ± 0.27	1.02 ± 0.22
Ship_related_SO ₂	0.69 ± 0.33	0.39 ± 0.12	0.30 ± 0.13	0.34 ± 0.16	0.53 ± 0.26	0.59 ± 0.20

Meteorological factors affect the dispersion, transport, accumulation, and chemical reactions of pollutants in the atmosphere. After normalizing for meteorological influences, the deweathered SO₂ concentrations (Deweathered_WSW and Deweathered_FDU) represent a time series with meteorological variability removed. These deweathered values is overall higher than the observed concentrations. Deweathered_FDU shows a decreasing trend in 2022 followed by a stabilization in 2023, while Deweathered_WSW exhibits a decline since 2018 and an increase again in 2022 and 2023. Nonetheless, under certain conditions, high concentrations of pollutants can still be locally transported, leading to elevated pollution levels, such as January in 2021. The Deweathered_FDU data, which represent the baseline SO₂ levels from terrestrial anthropogenic sources in urban Shanghai (mainly residential activities and ground transportation), showed a reduction of 16.7% (0.25 ppbv) over the six-year period. Due to the removal of meteorological dispersion effects, Deweathered_FDU exhibited a smoother U-shaped seasonal pattern, with lower concentrations in summer and higher concentrations in winter, consistent with previously observed trends in SO₂ vertical column densities over the Yangtze River Delta derived from satellite data (Wang et al., 2018). In contrast, the Deweathered_WSW results, which reflect the combined impact of both terrestrial and maritime SO₂ sources, retain some mid-year fluctuations. These fluctuations can be attributed to higher ship emissions during spring and summer (Fan et al., 2016; Jalkanen et al., 2009), as well as the influence of weather conditions, such as typhoons, which can restrict shipping activities.

The contribution of SO_2 air pollution directly associated with shipping activities (Ship_related_ SO_2) can be quantified by subtracting the Deweathered_FDU values from the Deweathered_WSW values. Over the six-year period, Ship_related_ SO_2 led to an average increase of 0.48 ± 0.25 ppbv in atmospheric SO_2 concentrations. Year-on-year reductions in Ship_related_ SO_2 were observed in 2019 and 2020, with declines of 43.47% and 23.08%, respectively. These reductions likely highlight the effectiveness of China's comprehensive low-sulfur policy within emission control areas, implemented on January 1, 2019, and the IMO global low-sulfur policy, enacted on January 1, 2020, in curbing SO_2 emissions from shipping

activities. From 2020 to 2023, Ship_related_SO₂ exhibited an average annual growth rate of 19.50%. This upward trend is plausibly attributable to the progressive increase in port throughput at Shanghai post-2020. The reasons behind these changes will be further discussed in Section 3.2.

Besides, the reduction in SO₂ levels not only improves air quality but will also mitigate the formation of sulfate aerosols, which are known to contribute to respiratory diseases and climate change. This highlights the dual benefits of low-sulfur policies for public health and environmental sustainability. To sustain these reductions, stricter enforcement of low-sulfur fuel regulations and enhanced monitoring of ship activities are recommended. Additionally, expanding emission control areas to other high-traffic regions could further mitigate the impact of ship emissions on coastal air quality.

3.2 Variation of SO₂-rich plumes in channel

250

255

260

To further investigate whether the observed increase in SO₂ concentrations in the shipping channel is attributable to the potential failure of low-sulfur policies, this study analyzes the frequency of SO₂ signals captured in the channel from 2018 to 2023, as well as changes in baseline levels. This analysis was conducted by separating high-time-resolution DOAS observations using the Baseline Estimation and Denoising using Sparsity (BEADs) algorithm (Ning et al., 2014), as illustrated in Fig. 5 (an example from January 12 to 13, 2018). The SO₂-rich plumes emitted during the operation of ships burning high-sulfur fuel can serve as indicators of the fuel's sulfur content, with higher plume peaks generally corresponding to higher sulfur levels. In contrast, lower variation in the baseline reflects the slower-changing trend of environmental SO₂, likely due to an increased proportion of low-emission vessels. All SO₂-rich plumes were confirmed by AIS data to originate from ship activity (Text S4).

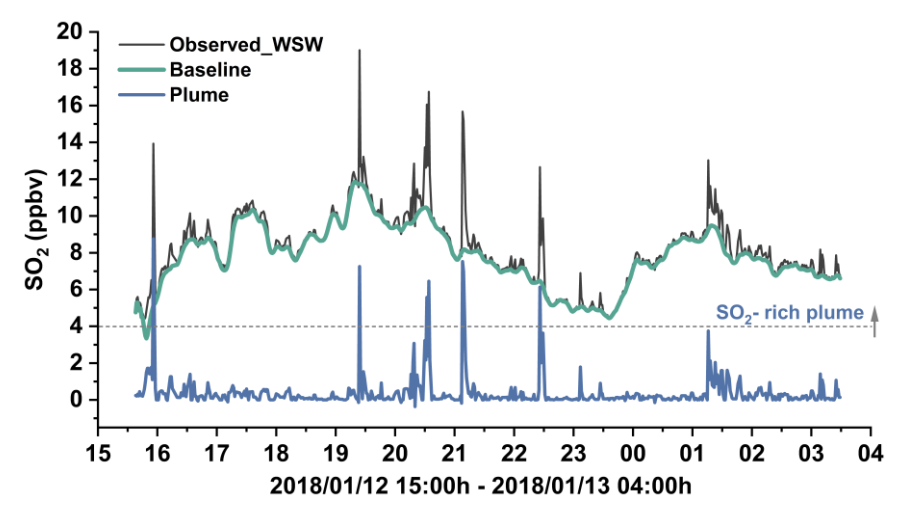


Figure 5: Time series of baseline trends and SO₂-rich plume signals separated from Observed_WSW using the BEADs algorithm. The black line represents the DOAS observed SO₂ concentrations, the green line indicates the baseline, and the blue line corresponds to plumes sequence extracted using the BEADs algorithm. The dashed line marks the threshold for identifying SO₂-rich plumes.

Figure 6 illustrates the annual variation in the absolute frequency proportion of SO₂-rich plume events, as well as changes in the baseline from 2018 to 2023. Here, SO₂-rich plumes are classified into six concentration ranges; [2,4) ppby, [4,6) ppby, [6,8) ppby, [8,10) ppby, [10,20) ppby, [20,30) ppby, respectively. The peak frequency of SO₂-rich plumes within the [6,30) ppby range exhibits a general declining trend year by year, while the numbers of major emission sources in the channel (cargo ships and passenger boats) exhibited a stable or growing trend from 2018 to 2023 (Fig. S12b). This demonstrates that 270 the observed trends in SO₂ emissions were not driven by changes in the scale or composition of the ship fleet (since emission sources were actually increasing), but rather by changes in the emission behavior of individual ships. These results indicate that low-sulfur policies have effectively reduced high-level SO₂ emissions from ships overall—particularly in 2023, when the SO₂ plumes exceeding 10 ppbv were nearly absent, despite gaps in observational data in certain years that caused fluctuations in the overall declining trend. In contrast, low SO₂ plumes [4,6) ppbv shows a fluctuating pattern, gradually increasing before 2020 and then declining with some variations during the policy stabilization phase. This trend may reflect the transitional effect of policy implementation: during the policy adjustment phase from 2018 to 2020, high SO₂ emissions began to decrease, but many pollution sources were not fully eliminated. Some ships may have started using fuels with slightly lower sulfur content, which led to an increase in the frequency of low SO₂ plumes. The adoption of low-sulfur fuels was the most common choice during this period, as it required little or no modification of existing engine systems (Vedachalam et al., 2022; Slaughter et al., 2020). In contrast, due to the high retrofitting costs of engine systems and the limited number of ships using LNG, most ports currently do not provide bunkering facilities for LNG and other alternative fuels, including biofuels (Vedachalam et al., 2022). Although scrubbers allowed the continued use of high-sulfur fuels, their application was constrained by high installation costs, long retrofitting times (up to 9 months) (Slaughter et al., 2020), and concerns about secondary environmental impacts from waste discharges (Hassell öv et al., 2013; Claremar et al., 2017; Thor et al., 2021). Only 3,000/60,000 vessels have been retrofitted with a scrubber system, as reported by Slaughter et al. (2020) As policies were more strictly enforced after 2020, the frequency of low SO₂ plumes emissions also started to decline, reflecting the impact of comprehensive control measures.

265

275

280

285

290

295

The baseline was highest in 2018 and subsequently exhibited a declining trend from 2018 to 2021, followed by an increase from 2021 to 2023, consistent with the variation in Ship_related_SO₂ observed in Section 3.1. During the policy adjustment period from 2018 to 2020, ships gradually reduced the sulfur content in their fuel, which led to an overall decrease in environmental SO₂, offsetting the increase in SO₂ emissions caused by the growing number of shipping activities. Starting in 2021, as policy implementation stabilized, the rise in the baseline was mainly attributed to the increased intensity of shipping operations. Therefore, we also analyzed the occurrence of low-concentration SO₂ plumes in the [2-4) ppbv range. These weaker plumes showed a clear increasing trend from 2021 to 2023, suggesting that the observed rise in baseline SO₂ was not driven by high-emission ships but rather by the cumulative contribution of numerous compliant vessels emitting smaller amounts of SO₂. The growing frequency of such plumes highlights how large-scale, compliant shipping activity can still elevate ambient SO₂ levels, especially when vessel density increases significantly.

Based on the combined results from Sections 3.1 and 3.2, it is likely that the observed increase in ambient SO₂ concentrations over shipping channel after 2020 was primarily driven by increased shipping activity. However, throughout the six years of observation, we consistently found signals suggesting the use of illegal fuel by ships (especially during the policy adjustment phase from 2018 to 2020). Given the expected continued growth in maritime activities, further reducing the sulfur content in marine fuels will be crucial to preventing Ship_related_SO₂ emissions from impacting air quality in coastal cities and potentially offsetting the land-based SO₂ reduction efforts already achieved. To address this, real-time monitoring systems, such as the DOAS-based approach developed in this study, could be integrated into port inspection protocols to identify and penalize non-compliant vessels more effectively. The methodology developed here provides a scalable framework for monitoring ship emissions in other coastal regions, enabling policymakers to better assess the effectiveness of low-sulfur policies and identify areas for improvement.

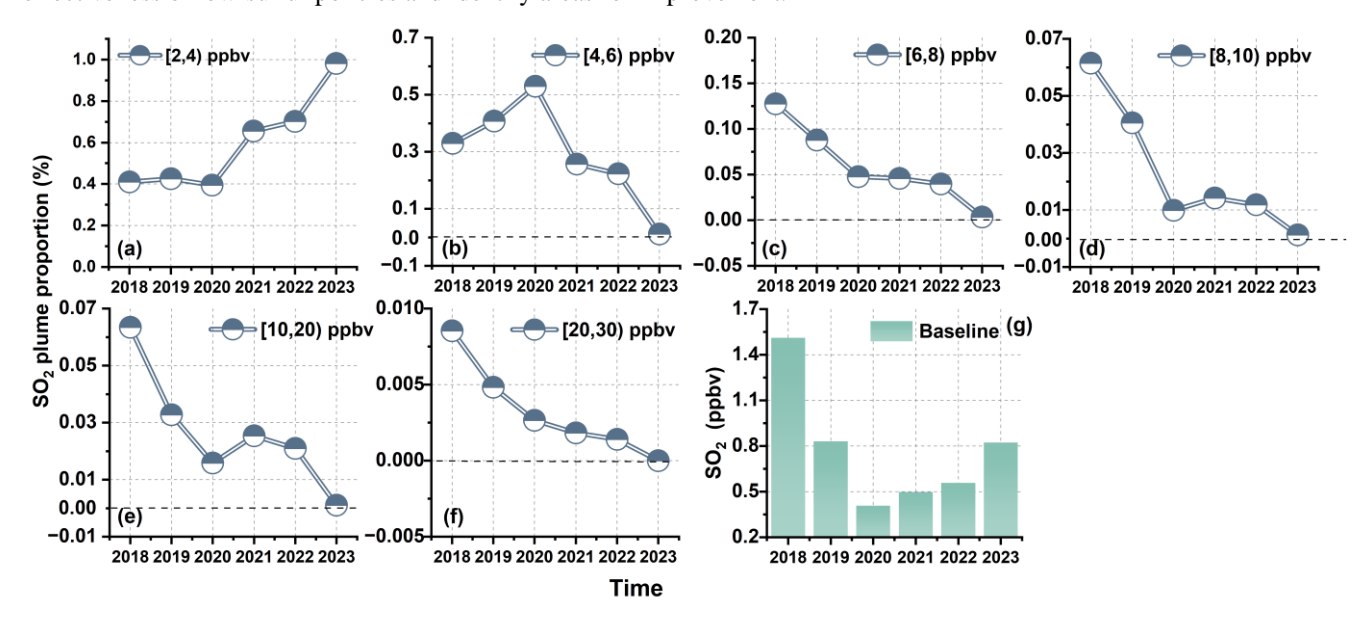


Figure 6: Yearly variation in SO₂ plume proportions and baseline level from 2018 to 2023. (a-f) Number of SO₂-rich plumes within different concentration ranges divided by the total valid spectra for each year. (g) Annual baseline concentrations of SO₂ obtained through the BEADs algorithm.

3.3 Variation of SO₂-rich plumes in channel

300

305

310

315

To determine which ships were potentially using non-compliant fuel, those SO₂-rich plumes identified in Section 3.2 were matched with ship information from AIS data. Given the high traffic density in the channel, multiple ships could be passing through the light path when a SO₂-rich plume was detected, therefore, two matching datasets were established as illustrated in Fig. 7: Unique-Matching Dataset: This dataset includes only those plumes where a single ship was present near the light path at the plume peak moment; Fastest-Matching Dataset: This dataset considers all plumes with identifiable concurrent ship activities and matches them with the ship that had the shortest time consumption when crossing the light path (indicating a higher likelihood of being the source). Approximately 30% of the plumes satisfied the strict criteria of Unique-

Matching dataset, emphasizing accuracy in source identification. In contrast, the Fastest-Matching dataset, while sacrificing some precision, provides a more comprehensive statistical representation of SO₂-rich plumes.

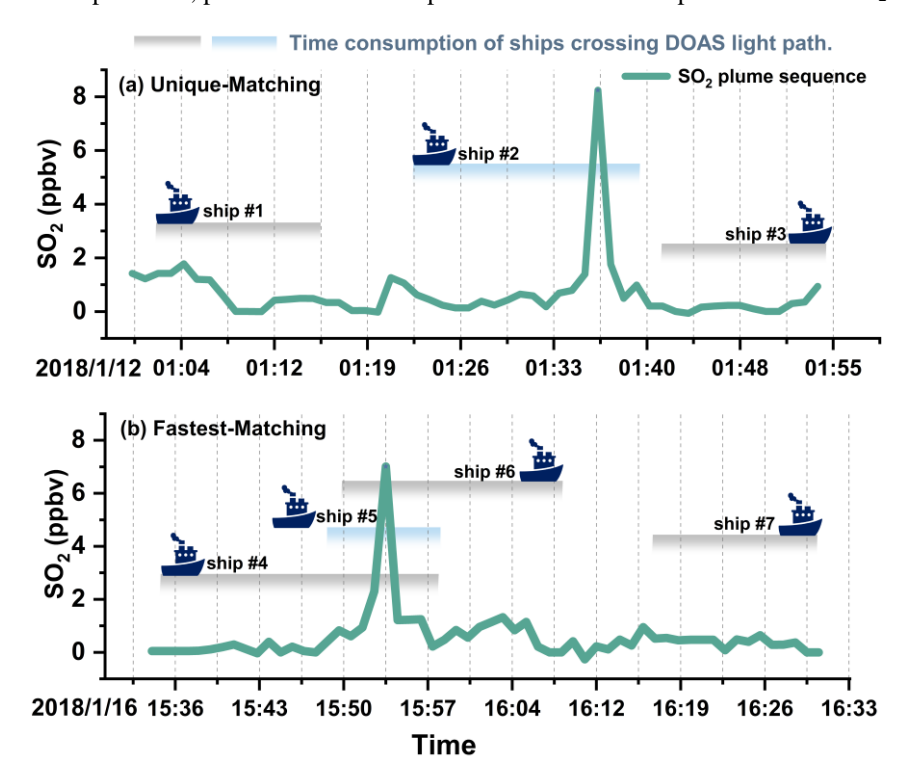


Figure 7: Illustration of two Matching-datasets for associating SO_2 -rich plumes with AIS ship activities. (a) Unique-Matching, where only plumes observed during the passage of a single ship (ship #2) near the DOAS light path are considered; and (b) Fastest-Matching, where plumes are matched to the ship (ship #5) with the shortest crossing time.

Figure 8 illustrates the proportional contributions of various ship types to different SO₂ peak value ranges within the Unique-Matching datasets during two distinct policy periods. During 2018–2020 in Fig. 8a, cargo ships dominated the contribution to SO₂ emissions across all peak value ranges, with proportions increasing from 56% in the >4 ppbv range to 80% in the >20 ppbv range. Passenger boats were the second-largest contributors, accounting for 29–31% in lower peak value ranges but decreasing as peak values increased. The contributions of oil tankers, fishing boats, and harbor ships were relatively small and remain stable across all ranges. During 2021–2023 in Fig. 8b, Cargo ships remain the primary contributors, with a slight decrease in dominance compared to 2018-2020, ranging from 55% in the >4 ppbv range to 60% in the >20 ppbv range. Although the proportion of peaks contributed by certain ship types increased, such as Passenger boats and harbor ships, the total peak occurrences for all ships significantly decreased during the policy stabilization period. At this stage, the distribution of ship types remains consistent regardless of changes in SO₂ plume concentrations. The same trend can be seen in the Fastest-Matching Dataset in Fig. S14. All results indicate that from 2018–2023, cargo ships consistently dominated SO₂ emissions under both Matching Datasets, particularly at higher plume value ranges. This suggests that greater emphasis should be placed on inspecting cargo ships for compliance with fuel standards during future port supervision and

enforcement efforts. Moreover, these non-compliant ship activities may have contributed to inaccuracies in bottom-up ship emission inventories based on AIS data during the 2018–2020 period (A comparison between observational data and AIS-based ship emission inventory is provided in Text S5).

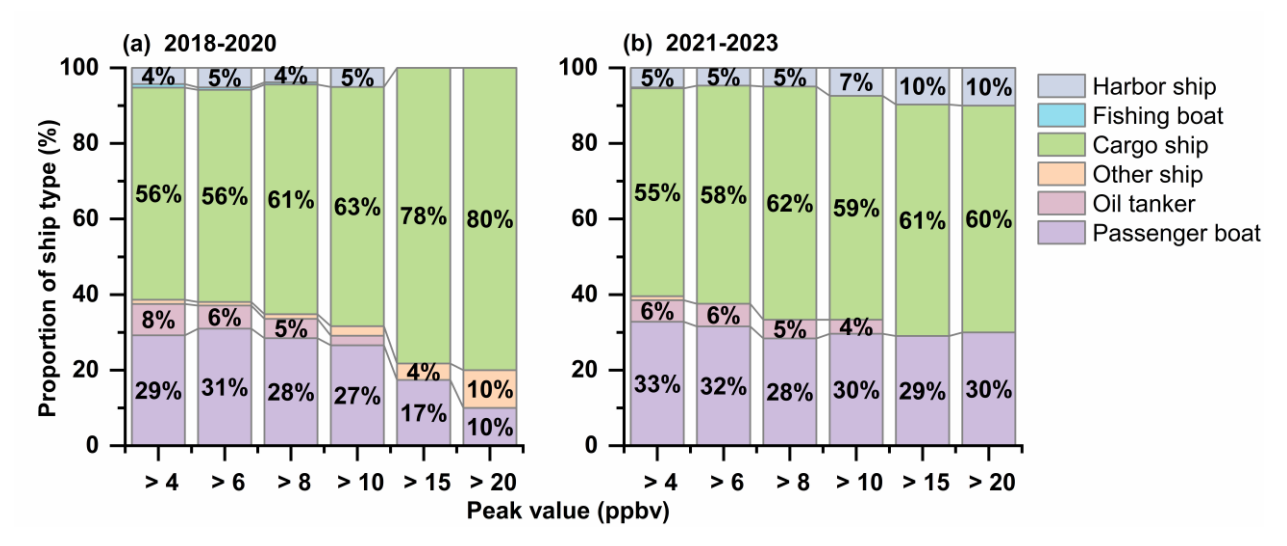


Figure 8: Proportional distribution of Unique-Matching ship types corresponding to different peak SO₂ values during (a) the policy adjustment period (2018–2020) and (b) the policy stabilization period (2021–2023). The ship types include harbor ships, fishing boats, cargo ships, passenger boats, oil tankers, and other ships.

4 Conclusion

340

345

350

360

This study provides a comprehensive six-year dataset on ship-related SO₂ emissions in the Shanghai shipping channel from 2018 to 2023, using continuous observations with Differential Optical Absorption Spectroscopy (DOAS) and machine learning techniques. The results indicate a marked decrease in urban SO₂ concentrations, reflecting the success of China's emission reduction policies. However, at the shipping channel, SO₂ levels initially decreased from 2018 to 2020 due to the low-sulfur policy but began to rise again from 2020 to 2023, driven by increased shipping activities. This underscores the need for stricter sulfur content regulations and better enforcement, particularly for non-compliant cargo ships, which were identified as key contributors to SO₂-rich plumes.

355 The study's findings highlight two important considerations for global policymakers: First, the success of low-sulfur policies in reducing emissions during the 2018–2020 phase offers valuable insights for other coastal nations, particularly those with rapidly growing maritime traffic. Second, the detection of non-compliant ships stresses the importance of enhancing real-time monitoring technologies.

The DOAS-based methodology employed here, which effectively separates ship emissions from meteorological and urban background influences, offers a scalable and cost-effective tool for port authorities worldwide. However, when expanding

this framework to other regions with varying maritime traffic densities and regulatory contexts, or when applying it to monitor additional pollutants such as NO_X and PM_{2.5}, it is imperative to acknowledge several methodological limitations. These include potential biases from the single-site background subtraction method, dependencies on meteorological reanalysis data in the Deweathered model, and uncertainties arising from vertical sampling geometry due to tidal variations and stack heights (detailed in Text S7). Although these systematic uncertainties do not substantially impact the conclusions supported by the large-sample data, they indicate that more precise data—such as using image recognition to determine specific ship activity and stack characteristics—would be necessary for finer-scale studies, such as quantifying emissions from individual ships. These factors should be carefully considered in future applications.

370 available. Data The data set of observation in this measurement report can be available at https://doi.org/DOI:10.17632/dvc97wxbcz.1 (Liu, 2025).

Author Contributions. J.L. conceived and designed the research. S.W., B.Z. and Y.Z. guided and supervised the research. S.Z. and Y.Y. guided the model construction. Z.H. provided AIS data. All authors participated in the discussion and interpretation of the data.

Competing interests. The contact author has declared that none of the authors has any competing interests.

Acknowledgements. This research has been supported by the National Natural Science Foundation of China (grant numbers 22376030, 22176037, 42375089 and 42077195). We would like to thank the Wusong Maritime Safety Bureau of Shanghai for the coordination of field measurements.

Financial support. This research has been supported by the National Natural Science Foundation of China (grant numbers 22376030, 22176037, 42375089 and 42077195).

385 **References**

- Ahmed, S., Li, T., Zhou, X. Y., Yi, P., Chen, R. J. R., and Reviews, S. E.: Quantifying the environmental footprints of biofuels for sustainable passenger ship operations, Renewable and Sustainable Energy Reviews 207, 114919, https://doi.org/10.1016/j.rser.2024.114919, 2025.
- Andreasen, A. and Mayer, S.: Use of Seawater Scrubbing for SO₂ Removal from Marine Engine Exhaust Gas, Energy & Fuels, 21, 3274-3279, http://10.1021/ef700359w, 2007.
 - Attah, E. E. and Bucknall, R. J. O. E.: An analysis of the energy efficiency of LNG ships powering options using the EEDI, Ocean Engineering, 110, 62-74, https://doi.org/10.1016/j.oceaneng.2015.09.040, 2015.

- Cai, S., Wang, Y., Zhao, B., Wang, S., Chang, X., and Hao, J.: The impact of the "Air Pollution Prevention and Control Action Plan" on PM2.5 concentrations in Jing-Jin-Ji region during 2012–2020, Science of The Total Environment, 580, 197-209, https://doi.org/10.1016/j.scitotenv.2016.11.188, 2017.
 - Carn, S. A., Clarisse, L., and Prata, A. J.: Multi-decadal satellite measurements of global volcanic degassing, Journal of Volcanology and Geothermal Research, 311, 99-134, https://doi.org/10.1016/j.jvolgeores.2016.01.002, 2016.
- Ceballos-Santos, S., Gonz áez-Pardo, J., Carslaw, D. C., Santurt ún, A., Santib áñez, M., and Fern ández-Olmo, I.:

 Meteorological Normalisation Using Boosted Regression Trees to Estimate the Impact of COVID-19 Restrictions on
 Air Quality Levels, International journal of environmental research and public health, 18,
 http://doi.org/10.3390/ijerph182413347, 2021.
 - Cesilla de Souza, L. and Eugânio Abel Seabra, J.: Technical-economic and environmental assessment of marine biofuels produced in Brazil, Cleaner Environmental Systems, 13, 100195, https://doi.org/10.1016/j.cesys.2024.100195, 2024.
- Cheng, Y., Wang, S., Zhu, J., Guo, Y., Zhang, R., Liu, Y., Zhang, Y., Yu, Q., Ma, W., and Zhou, B.: Surveillance of SO2 and NO2 from ship emissions by MAX-DOAS measurements and the implications regarding fuel sulfur content compliance, Atmos. Chem. Phys., 19, 13611-13626, http://doi.org/10.5194/acp-19-13611-2019, 2019.
 - Claremar, B., Haglund, K., and Rutgersson, A.: Ship emissions and the use of current air cleaning technology: contributions to air pollution and acidification in the Baltic Sea, Earth Syst. Dynam., 8, 901-919, http://10.5194/esd-8-901-2017, 2017.
 - Ducruet, C. and Wang, L.: China's Global Shipping Connectivity: Internal and External Dynamics in the Contemporary Era (1890–2016), Chinese Geographical Science, 28, 202-216, http://doi.org/10.1007/s11769-018-0942-x, 2018.

- Eger, P., Mathes, T., Zavarsky, A., and Duester, L.: Measurement report: Inland ship emissions and their contribution to NOx and ultrafine particle concentrations at the Rhine, Atmos. Chem. Phys., 23, 8769-8788, http://doi.org/10.5194/acp-23-8769-2023, 2023.
- Fan, Q., Zhang, Y., Ma, W., Ma, H., Feng, J., Yu, Q., Yang, X., Ng, S. K. W., Fu, Q., and Chen, L.: Spatial and Seasonal Dynamics of Ship Emissions over the Yangtze River Delta and East China Sea and Their Potential Environmental Influence, Environmental Science & Technology, 50, 1322-1329, http://doi.org/10.1021/acs.est.5b03965, 2016.
 - Feng, J., Zhang, Y., Li, S., Mao, J., Patton, A. P., Zhou, Y., Ma, W., Liu, C., Kan, H., Huang, C., An, J., Li, L., Shen, Y., Fu, Q., Wang, X., Liu, J., Wang, S., Ding, D., Cheng, J., Ge, W., Zhu, H., and Walker, K.: The influence of spatiality on shipping emissions, air quality and potential human exposure in the Yangtze River Delta/Shanghai, China, Atmos. Chem. Phys., 19, 6167-6183, http://doi.org/10.5194/acp-19-6167-2019, 2019a.
 - Feng, X., Ma, Y., Lin, H., Fu, T.-M., Zhang, Y., Wang, X., Zhang, A., Yuan, Y., Han, Z., Mao, J., Wang, D., Zhu, L., Wu, Y., Li, Y., and Yang, X.: Impacts of Ship Emissions on Air Quality in Southern China: Opportunistic Insights from the Abrupt Emission Changes in Early 2020, Environmental Science & Technology, 57, 16999-17010, http://doi.org/10.1021/acs.est.3c04155, 2023.
- Feng, Y., Ning, M., Lei, Y., Sun, Y., Liu, W., and Wang, J.: Defending blue sky in China: Effectiveness of the "Air Pollution Prevention and Control Action Plan" on air quality improvements from 2013 to 2017, Journal of Environmental Management, 252, 109603, https://doi.org/10.1016/j.jenvman.2019.109603, 2019b.
- Fossum, K. N., Lin, C., O'Sullivan, N., Lei, L., Hellebust, S., Ceburnis, D., Afzal, A., Tremper, A., Green, D., Jain, S., Byčenkienė, S., O'Dowd, C., Wenger, J., and Ovadnevaite, J.: Two distinct ship emission profiles for organic-sulfate source apportionment of PM in sulfur emission control areas, EGUsphere, 2024, 1-26, http://doi.org/10.5194/egusphere-2024-1262, 2024.
 - Friedman, J. H.: Stochastic gradient boosting, Computational Statistics & Data Analysis, 38, 367-378, https://doi.org/10.1016/S0167-9473(01)00065-2, 2002.

- Gall, J., Yao, A., Razavi, N., Gool, L. V., and Lempitsky, V.: Hough Forests for Object Detection, Tracking, and Action Recognition, IEEE Transactions on Pattern Analysis and Machine Intelligence, 33, 2188-2202, http://doi.org/10.1109/TPAMI.2011.70, 2011.
 - Ghanbari Ghozikali, M., Heibati, B., Naddafi, K., Kloog, I., Oliveri Conti, G., Polosa, R., and Ferrante, M.: Evaluation of Chronic Obstructive Pulmonary Disease (COPD) attributed to atmospheric O₃, NO₂, and SO₂ using Air Q Model (2011-2012 year), Environmental research, 144, 99-105, http://doi.org/10.1016/j.envres.2015.10.030, 2016.
- 440 Grange, S. K. and Carslaw, D. C.: Using meteorological normalisation to detect interventions in air quality time series, Science of The Total Environment, 653, 578-588, https://doi.org/10.1016/j.scitotenv.2018.10.344, 2019.
 - Grange, S. K., Carslaw, D. C., Lewis, A. C., Boleti, E., and Hueglin, C.: Random forest meteorological normalisation models for Swiss PM10 trend analysis, Atmos. Chem. Phys., 18, 6223-6239, http://doi.org/10.5194/acp-18-6223-2018, 2018.
- Gu, C., Wang, S., Zhu, J., Wu, S., Duan, Y., Gao, S., and Zhou, B.: Investigation on the urban ambient isoprene and its oxidation processes, Atmospheric Environment, 270, 118870, https://doi.org/10.1016/j.atmosenv.2021.118870, 2022.
 - Guo, Y., Wang, S., Gao, S., Zhang, R., Zhu, J., and Zhou, B.: Influence of ship direct emission on HONO sources in channel environment, Atmospheric Environment, 242, 117819, https://doi.org/10.1016/j.atmosenv.2020.117819, 2020.
 - Hassellöv, I.-M., Turner, D. R., Lauer, A., and Corbett, J. J.: Shipping contributes to ocean acidification, Geophysical Research Letters, 40, 2731-2736, https://doi.org/10.1002/grl.50521, 2013.
 - Hersbach, H., Bell, B., Berrisford, P., Hirahara, S., Horányi, A., Muñoz Sabater, J., Nicolas, J., Peubey, C., Radu, R., Schepers, D., Simmons, A., Soci, C., Abdalla, S., Abellan, X., Balsamo, G., Bechtold, P., Biavati, G., Bidlot, J., Bonavita, M., and Thépaut, J. N.: The ERA5 global reanalysis, Quarterly Journal of the Royal Meteorological Society, 146, http://10.1002/qj.3803, 2020.
- Jalkanen, J. P., Brink, A., Kalli, J., Pettersson, H., Kukkonen, J., and Stipa, T.: A modelling system for the exhaust emissions of marine traffic and its application in the Baltic Sea area, Atmos. Chem. Phys., 9, 9209-9223, http://doi.org/10.5194/acp-9-9209-2009, 2009.
 - Kattner, L., Mathieu-Üffing, B., Burrows, J. P., Richter, A., Schmolke, S., Seyler, A., and Wittrock, F.: Monitoring compliance with sulfur content regulations of shipping fuel by in situ measurements of ship emissions, Atmos. Chem. Phys., 15, 10087-10092, http://doi.org/10.5194/acp-15-10087-2015, 2015.
 - Krause, K., Wittrock, F., Richter, A., Schmitt, S., Pöhler, D., Weigelt, A., and Burrows, J. P.: Estimation of ship emission rates at a major shipping lane by long-path DOAS measurements, Atmos. Meas. Tech., 14, 5791-5807, http://doi.org/10.5194/amt-14-5791-2021, 2021.
 - Kuttippurath, J.: Environ. Sci. Pollut. Res., 29, http://doi.org/10.1007/s11356-022-21319-2, 2022.

460

- Li, J., Wang, S., Yang, T., Zhang, S., Zhu, J., Xue, R., Liu, J., Li, X., Ge, Y., and Zhou, B.: Investigating the causes and reduction approaches of nocturnal ozone increase events over Tai'an in the North China Plain, Atmospheric Research, 307, 107499, https://doi.org/10.1016/j.atmosres.2024.107499, 2024.
 - Li, S., Zhang, Y., Zhao, J., Sarwar, G., Zhou, S., Chen, Y., Yang, G., and Saiz-Lopez, A.: Regional and Urban-Scale Environmental Influences of Oceanic DMS Emissions over Coastal China Seas, http://doi.org/10.3390/atmos11080849, 2020.
 - Liu, J., Wang, S., Zhang, Y., Yan, Y., Zhu, J., Zhang, S., Wang, T., Tan, Y., and Zhou, B.: Investigation of formaldehyde sources and its relative emission intensity in shipping channel environment, Journal of Environmental Sciences, 142, 142-154, https://doi.org/10.1016/j.jes.2023.06.020, 2024.
- Liu, Z., Lu, X., Feng, J., Fan, Q., Zhang, Y., and Yang, X.: Influence of Ship Emissions on Urban Air Quality: A
 Comprehensive Study Using Highly Time-Resolved Online Measurements and Numerical Simulation in Shanghai,
 Environmental Science & Technology, 51, 202-211, http://doi.org/10.1021/acs.est.6b03834, 2017.

- Lou, L., Li, J., and Zhong, S.: Sulfur dioxide (SO2) emission reduction and its spatial spillover effect in high-tech industries: based on panel data from 30 provinces in China, Environmental Science and Pollution Research, 28, 31340-31357, http://doi.org/10.1007/s11356-021-12755-7, 2021.
- Lunde Hermansson, A., Hassellöv, I.-M., Grönholm, T., Jalkanen, J.-P., Fridell, E., Parsmo, R., Hassellöv, J., and Ytreberg, E.: Strong economic incentives of ship scrubbers promoting pollution, Nature Sustainability, 7, 812-822, http://doi.10.1038/s41893-024-01347-1, 2024.
 - Luo, Z., Lv, Z., Zhao, J., Sun, H., He, T., Yi, W., Zhang, Z., He, K., and Liu, H.: Shipping-related pollution decreased but mortality increased in Chinese port cities, Nature Cities, 1, 295-304, http://doi.org/10.1038/s44284-024-00050-8, 2024.
- - Meyer, A. and Pac, G.: Analyzing the characteristics of plants choosing to opt-out of the Large Combustion Plant Directive, Utilities Policy, 45, 61-68, https://doi.org/10.1016/j.jup.2017.02.001, 2017.
- 490 Miller, B. G.: 8 Coal-Fired Emissions and Legislative Action, in: Clean Coal Engineering Technology, edited by: Miller, B. G., Butterworth-Heinemann, Boston, 301-374, https://doi.org/10.1016/B978-1-85617-710-8.00008-X, 2011.
 - Mohiuddin, K., Akram, M. N., Islam, M. M., Shormi, M. E., and Wang, X.: Exploring the trends of research: a bibliometric analysis of global ship emission estimation practices, Journal of Ocean Engineering and Marine Energy, http://doi.org/10.1007/s40722-024-00341-1, 2024.
- Moran, M. D.: Application of a Comprehensive Acid Deposition Model in Support of Acid Rain Abatement in Canada, Air Pollution Modeling and Its Application XVII, Boston, MA, 2007, 109-118, http://doi.org/10.1007/978-0-387-68854-113,
 - Ning, X., Selesnick, I. W., and Duval, L.: Chromatogram baseline estimation and denoising using sparsity (BEADS), Chemometrics and Intelligent Laboratory Systems, 139, 156-167, https://doi.org/10.1016/j.chemolab.2014.09.014, 2014.
- Pan, B.: Application of XGBoost algorithm in hourly PM_{2.5} concentration prediction, IOP Conference Series: Earth and Environmental Science, 113, 012127, http://doi.org/10.1088/1755-1315/113/1/012127, 2018.
 - Pavlenko, N., Comer, B., Zhou, Y., Clark, N., and Rutherford, D. J. S. E. P. A. S., Sweden: The climate implications of using LNG as a marine fuel, Swedish Environmental Protection Agency: Stockholm, 2020.
- Shi, J., Zhu, Y., Feng, Y., Yang, J., and Xia, C. J. A.: A prompt decarbonization pathway for shipping: green hydrogen, ammonia, and methanol production and utilization in marine engines, Atmosphere, 14, 584, https://doi.org/10.3390/atmos14030584, 2023.
 - Slaughter, A., Ray, S., and Shattuck, T. J. D. D. L.: International Maritime Organization (IMO) 2020 strategies in a non-compliant world, 1-14, 2020.
- Squizzato, S., Masiol, M., Rich, D. Q., and Hopke, P. K.: A long-term source apportionment of PM_{2.5} in New York State during 2005–2016, Atmospheric Environment, 192, 35-47, https://doi.org/10.1016/j.atmosenv.2018.08.044, 2018.
 - Svanberg, M., Ellis, J., Lundgren, J., Land av, I. J. R., and Reviews, S. E.: Renewable methanol as a fuel for the shipping industry, Renewable and Sustainable Energy Reviews, 94, 1217-1228, https://doi.org/10.1016/j.rser.2018.06.058, 2018.
 - Thor, P., Granberg, M. E., Winnes, H., and Magnusson, K.: Severe Toxic Effects on Pelagic Copepods from Maritime Exhaust Gas Scrubber Effluents, Environmental Science & Technology, 55, 5826-5835, http://doi.org/10.1021/acs.est.0c07805, 2021.

Tu, E., Zhang, G., Rachmawati, L., Rajabally, E., and Huang, G. B.: Exploiting AIS Data for Intelligent Maritime Navigation: A Comprehensive Survey From Data to Methodology, IEEE Transactions on Intelligent Transportation Systems, 19, 1559-1582, http://doi.org/10.1109/TITS.2017.2724551, 2018.

- Van Aardenne, J. A., Dentener, F. J., Olivier, J. G. J., Goldewijk, C. G. M. K., and Lelieveld, J.: A 1 °×1 ° resolution data set of historical anthropogenic trace gas emissions for the period 1890–1990, Global Biogeochemical Cycles, 15, 909-928, https://doi.org/10.1029/2000GB001265, 2001.
 - Vedachalam, S., Baquerizo, N., and Dalai, A. K.: Review on impacts of low sulfur regulations on marine fuels and compliance options, Fuel, 310, 122243, https://doi.org/10.1016/j.fuel.2021.122243, 2022.
- Viana, M., Hammingh, P., Colette, A., Querol, X., Degraeuwe, B., Vlieger, I. d., and van Aardenne, J.: Impact of maritime transport emissions on coastal air quality in Europe, Atmospheric Environment, 90, 96-105, https://doi.org/10.1016/j.atmosenv.2014.03.046, 2014.
 - von Nieding, G.: Possible mutagenic properties and carcinogenic action of the irritant gaseous pollutants NO2, O3, and SO2, Environmental health perspectives, 22, 91-92, http://doi.org/10.1289/ehp.782291, 1978.
- Vu, T. V., Shi, Z., Cheng, J., Zhang, Q., He, K., Wang, S., Harrison, R. M. J. A. C., and Physics: Assessing the impact of clean air action on air quality trends in Beijing using a machine learning technique, Atmos. Chem. Phys., https://doi.org/10.5194/acp-19-11303-2019, 2019.
 - Wang, T., Wang, P., Theys, N., Tong, D., Hendrick, F., Zhang, Q., and Van Roozendael, M.: Spatial and temporal changes in SO2 regimes over China in the recent decade and the driving mechanism, Atmos. Chem. Phys., 18, 18063-18078, http://doi.org/10.5194/acp-18-18063-2018, 2018.
- Wang, X., Shen, Y., Lin, Y., Pan, J., Zhang, Y., Louie, P. K. K., Li, M., and Fu, Q.: Atmospheric pollution from ships and its impact on local air quality at a port site in Shanghai, Atmos. Chem. Phys., 19, 6315-6330, http://doi.org/10.5194/acp-19-6315-2019, 2019.
- Wang, X., Yi, W., Lv, Z., Deng, F., Zheng, S., Xu, H., Zhao, J., Liu, H., and He, K.: Ship emissions around China under gradually promoted control policies from 2016 to 2019, Atmos. Chem. Phys., 21, 13835-13853, http://doi.org/10.5194/acp-21-13835-2021, 2021.
 - Xiao, G., Wang, T., Chen, X., and Zhou, L.: Evaluation of Ship Pollutant Emissions in the Ports of Los Angeles and Long Beach, http://doi.org/10.3390/jmse10091206, 2022.
 - Xiao, G., Wang, T., Luo, Y., and Yang, D.: Analysis of port pollutant emission characteristics in United States based on multiscale geographically weighted regression, Frontiers in Marine Science, 10, http://doi.org/10.3389/fmars.2023.1131948, 2023.

- Yang, D., Wu, L., Wang, S., Jia, H., and Li, K. X.: How big data enriches maritime research a critical review of Automatic Identification System (AIS) data applications, Transport Reviews, 39, 755-773, https://doi.org/10.1080/01441647.2019.1649315, 2019.
- Yue, H., He, C., Huang, Q., Yin, D., and Bryan, B. A.: Stronger policy required to substantially reduce deaths from PM2.5 pollution in China, Nature Communications, 11, 1462, http://doi.org/10.1038/s41467-020-15319-4, 2020.
 - Zhang, S., Wang, S., Xue, R., Zhu, J., Tanvir, A., Li, D., and Zhou, B.: Impact Assessment of COVID-19 Lockdown on Vertical Distributions of NO₂ and HCHO From MAX-DOAS Observations and Machine Learning Models, Journal of Geophysical Research: Atmospheres, 127, e2021JD036377, https://doi.org/10.1029/2021JD036377, 2022.
- Zhang, X., van der A, R., Ding, J., Zhang, X., and Yin, Y.: Significant contribution of inland ships to the total NOx emissions along the Yangtze River, Atmos. Chem. Phys., 23, 5587-5604, http://doi.org/10.5194/acp-23-5587-2023, 2023.
 - Zhang, X., Zhang, Y., Liu, Y., Zhao, J., Zhou, Y., Wang, X., Yang, X., Zou, Z., Zhang, C., Fu, Q., Xu, J., Gao, W., Li, N., and Chen, J.: Changes in the SO₂ Level and PM_{2.5} Components in Shanghai Driven by Implementing the Ship Emission Control Policy, Environmental Science & Technology, 53, 11580-11587, http://doi.org/10.1021/acs.est.9b03315, 2019.

Zhang, Y., Yang, X., Brown, R., Yang, L., Morawska, L., Ristovski, Z., Fu, Q., and Huang, C.: Shipping emissions and their impacts on air quality in China, Science of The Total Environment, 581-582, 186-198, https://doi.org/10.1016/j.scitotenv.2016.12.098, 2017.

565

575

- Zhao, J., Zhang, Y., Patton, A. P., Ma, W., Kan, H., Wu, L., Fung, F., Wang, S., Ding, D., and Walker, K.: Projection of ship emissions and their impact on air quality in 2030 in Yangtze River delta, China, Environmental Pollution, 263, 114643, https://doi.org/10.1016/j.envpol.2020.114643, 2020.
 - Zhong, Q., Shen, H., Yun, X., Chen, Y., Ren, Y. a., Xu, H., Shen, G., Ma, J., and Tao, S.: Effects of International Fuel Trade on Global Sulfur Dioxide Emissions, Environmental Science & Technology Letters, 6, 727-731, http://doi.org/10.1021/acs.estlett.9b00617, 2019.
- Zhu, J., Wang, S., Zhang, S., Xue, R., Gu, C., and Zhou, B.: Changes in NO₃ Radical and Its Nocturnal Chemistry in Shanghai From 2014 to 2021 Revealed by Long-Term Observation and a Stacking Model: Impact of China's Clean Air Action Plan, Journal of Geophysical Research: Atmospheres, 127, e2022JD037438, https://doi.org/10.1029/2022JD037438, 2022.
 - Zhu, J., Wang, S., Wang, H., Jing, S., Lou, S., Saiz-Lopez, A., and Zhou, B.: Observationally constrained modeling of atmospheric oxidation capacity and photochemical reactivity in Shanghai, China, Atmos. Chem. Phys., 20, 1217-1232, http://doi.org/10.5194/acp-20-1217-2020, 2020.
 - Zis, T., North, R. J., Angeloudis, P., Ochieng, W. Y., and Bell, M. G. J. T. R. R.: Environmental balance of shipping emissions reduction strategies, Transportation Research Record Journal of the Transportation Research Board, 2479, 25-33, http://doi.org/10.3141/2479-04, 2015.
- Zis, T., North, R. J., Angeloudis, P., Ochieng, W. Y., Harrison Bell, M. G. J. M. E., and Logistics: Evaluation of cold ironing and speed reduction policies to reduce ship emissions near and at ports, Maritime Economics & Logistics, 16, 371-398, http://doi.org/10.1057/mel.2014.6, 2014.
 - Zou, Z., Zhao, J., Zhang, C., Zhang, Y., Yang, X., Chen, J., Xu, J., Xue, R., and Zhou, B.: Effects of cleaner ship fuels on air quality and implications for future policy: A case study of Chongming Ecological Island in China, Journal of Cleaner Production, 267, 122088, https://doi.org/10.1016/j.jclepro.2020.122088, 2020.